JOURNAL OF GEOPHYSICAL RESEARCH, VOL. 115, D00K07, doi:10.1029/2009JD012893, 2010

Identification of sources and formation processes of atmospheric sulfate by sulfur isotope and scanning electron microscope measurements

Zhaobing Guo,[1,2] Zhanqing Li,[1,2,3] James Farquhar,[4] Alan J. Kaufman,[4] Nanping Wu,[4] Can Li,[2] Russell R. Dickerson,[2] and Pucai Wang[3]

Received 24 July 2009; revised 12 November 2009; accepted 10 December 2009; published 28 April 2010.

[1] Atmospheric sulfate aerosols have a cooling effect on the Earth's surface and can change cloud microphysics and precipitation. China has heavy loading of sulfate, but their sources and formation processes remain uncertain. In this study we characterize possible sources and formation processes of atmospheric sulfate by analyzing sulfur isotope abundances (^{32}S, ^{33}S, ^{34}S, and ^{36}S) and by detailed X-ray diffraction and scanning electron microscope (SEM) imaging of aerosol samples acquired at a rural site in northern China from March to August 2005. The comparison of SEM images from coal fly ash and the atmospheric aerosols suggests that direct emission from coal combustion is a substantial source of primary atmospheric sulfate in the form of $CaSO_4$. Airborne gypsum ($CaSO_4 \cdot 2H_2O$) is usually attributed to eolian dust or atmospheric reactions with H_2SO_4. SEM imaging also reveals mineral particles with soot aggregates adhered to the surface where they could decrease the single scattering albedo of these aerosols. In summer months, heterogeneous oxidation of SO_2, derived from coal combustion, appears to be the dominant source of atmospheric sulfate. Our analyses of aerosol sulfate show a seasonal variation in $\Delta^{33}S$ ($\Delta^{33}S$ describes either a ^{33}S excess or depletion relative to that predicted from consideration of classical mass-dependent isotope effects). Similar sulfur isotope variations have been observed in other atmospheric samples and in (homogenous) gas-phase reactions. On the basis of atmospheric sounding and satellite data as well as a possible relationship between $\Delta^{33}S$ and Convective Available Potential Energy (CAPE) during the sampling period, we attribute the sulfur isotope anomalies ($\Delta^{33}S$ and $\Delta^{36}S$) in Xianghe aerosol sulfates to another atmospheric source (upper troposphere or lower stratosphere).

Citation: Guo, Z., Z. Li, J. Farquhar, A. J. Kaufman, N. Wu, C. Li, R. R. Dickerson, and P. Wang (2010), Identification of sources and formation processes of atmospheric sulfate by sulfur isotope and scanning electron microscope measurements, *J. Geophys. Res.*, *115*, D00K07, doi:10.1029/2009JD012893.

1. Introduction

[2] The abundance and radiative properties of atmospheric aerosols represent an internal forcing mechanism for climate change and one of the most uncertain factors of the Earth's climate system [*Intergovernmental Panel on Climate Change*, 2007]. Anthropogenic aerosol loading in China has drastically increased over the last few decades, and may have a strong impact on regional climate [*Li*, 2004]. Heavy aerosol loading can affect the energy balance [*Z. Li et al.*, 2007a] and the evolution of the planetary boundary layer [*Yu et al.*, 2002]. High absorbance of solar radiation by Asian aerosol has been attributed to internal mixing [e.g., *Chameides et al.*, 1999; *Höller et al.*, 2003; *Clarke et al.*, 2004; *Cheng et al.*, 2009] and/or soot adhered to the surface of mineral dust particles [*Chaudhry et al.*, 2007; *Chaudhry*, 2008]. In addition, aerosols have been related to the recent weakening of the East Asian summer monsoon [*Xu et al.*, 2006], reduced cloudiness [*Qian et al.*, 2006] and the "north drought south flood" climate anomaly [*Xu*, 2001] over China.

[3] One of the prevalent components of particulate matter in China is sulfate; investigations of sulfur isotopes (^{32}S, ^{33}S, ^{34}S and ^{36}S) in aerosols have the potential to be useful for understanding sources and formation processes. Sulfur isotope compositions are measured in terms of delta values (δ), defined as

$$\delta^i S = \left[\left({}^iS/{}^{32}S \right)_{\text{aerosol}} / \left({}^iS/{}^{32}S \right)_{\text{reference}} - 1 \right] \times 1000, \quad (1)$$

[1]School of Environmental Science and Engineering, Nanjing University of Information Science and Technology, Nanjing, China.
[2]ESSIC and Department of Atmospheric and Oceanic Science, University of Maryland, College Park, Maryland, USA.
[3]Institute of Atmospheric Physics, Chinese Academy of Sciences, Beijing, China.
[4]ESSIC and Department of Geology, University of Maryland, College Park, Maryland, USA.

0148-0227/10/2009JD012893

where ^{i}S is ^{33}S, ^{34}S or ^{36}S. The delta values represent the deviation of the ratio of the abundance of a rare sulfur isotope in samples relative to the same ratio in an international reference material: Vienna-Canyon Diablo Troilite (V-CDT) [*Ding et al.*, 2001]. Classical isotope effects and a number of kinetic isotope effects (KIE) have a strong dependence on relative mass differences between the isotopes yielding relationships for the stable isotopes given by $\delta^{33}S \approx 0.515 \times \delta^{34}S$ and $\delta^{36}S \approx 1.90 \times \delta^{34}S$, which are often referred to as mass-dependent [e.g., *Hulston and Thode*, 1965]. Some types of isotope effects, however, (including some KIEs), have dependences on properties other than mass. These include, but are not limited to, electron spin (magnetic isotope effects), the symmetry of isotopic species involved in reactions, nuclear volume effects, and level matching between states, which are recognized as important in gas-phase reactions occurring in the atmosphere. In these cases, the $\delta^{33}S$ and $\delta^{36}S$ data may deviate from mass-dependent relationships and these are referred to as having mass-independent or non-mass-dependent isotope compositions. To describe and distinguish between mass-dependent and mass-independent isotope compositions, the capital delta notation ($\Delta^{33}S$ and $\Delta^{36}S$) is used, where

$$\Delta^{33}S = \delta^{33}S - \left[\left(\delta^{34}S/1000 + 1\right)^{0.515} - 1\right] \times 1000 \quad (2)$$

$$\Delta^{36}S = \delta^{36}S - \left[\left(\delta^{34}S/1000 + 1\right)^{1.90} - 1\right] \times 1000. \quad (3)$$

This notation describes the excess or deficiency of ^{33}S or ^{36}S relative to a reference "mass-dependent" fractionation array.

[4] Sulfur isotopes have been traditionally used to identify and characterize the sources of sulfur in the atmosphere because sources such as anthropogenic SO_2, biogenic sulfur, and sulfur from airborne particulate matter (dust and mineral matter) often possesses different $\delta^{34}S$ values [*Nielsen*, 1974; *Kawamura et al.*, 2001; *Norman et al.*, 1999; *Novak et al.*, 2001; *Ono et al.*, 2009; *Lyons*, 2009; *Szynkiewicz et al.*, 2009]. The sulfur isotopes in atmospheric aerosols over China have been observed to be similar to those in coal combusted in the region [*Mukai et al.*, 2001]. It has also been recognized that sulfur isotope data may be a useful tool for evaluating the oxidation reaction pathways of SO_2 [*Norman et al.*, 2006; *Winterholler et al.*, 2008] and in analyzing the contribution of atmospheric pollutants into groundwater and the transport of contaminants in the environment [*Torfs and Van Grieken*, 1997; *Toyama et al.*, 2007; *Li et al.*, 2006].

[5] The possible occurrence of mass-dependent and mass-independent isotope compositions is recognized as having the potential to provide a finer resolution means to identify the sources, sinks, and processing of sulfur in the atmosphere. For instance, *Romero and Thiemens* [2003] measured multiple sulfur isotope compositions in the present atmosphere from samples of North Hemisphere aerosol sulfate and found mass-independent sulfur isotope anomalies, which they attributed to stratospheric input of sulfate produced from photochemical reactions. It has been suggested that UV photooxidation in the stratosphere can leave a characteristic $\Delta^{33}S$ signature [*Savarino et al.*, 2003].

[6] In this study, multisulfur isotope compositions in aerosol samples from Xianghe, China are measured in different seasons. Taking into account meteorological factors and satellite data, we discuss how multiple sulfur isotopic signatures may be produced in today's atmosphere and how they end up as airborne particles that affect radiative balance near Earth's surface.

2. Field and Laboratory Experiments

[7] In order to gain a basic knowledge of the characteristics of aerosols and trace gases and an understanding of their climatic effects, the East Asian Studies of Tropospheric Aerosols: an International Regional Experiment (EAST-AIRE) was established as a U.S.-China joint research endeavor to (1) acquire and understand the physical, chemical and optical properties of dominant natural and anthropogenic aerosols and their precursor gases in China and (2) gain insights into the direct and indirect effects of these aerosols on radiation, cloud, precipitation, atmospheric circulation and the environment.

[8] A focus of the EAST-AIRE was placed on obtaining in situ measurements of aerosols and pollutant gases near or downwind of major source regions throughout inland China. Both routine and intensive observation campaigns (IOC) have been conducted utilizing ground-based and airborne measurements [*Z. Li et al.*, 2007b]. Following outdoor field campaigns, a battery of observational and geochemical tests were conducted to evaluate the major sources of pollutants. Below we provide brief descriptions of these procedures.

2.1. Outdoor Aerosol Sampling

[9] Aerosol samples were acquired at one of the EAST-AIRE super sites located in Xianghe (39.75°N, 116.96°E; 35 m above sea level), about 70 km east-southeast and generally downwind of the Beijing metropolitan area. A high-volume aerosol sampler was used to collect particles (total aerosols without size cut) on Whatman Grade No. 41 quantitative filter papers [*Prospero et al.*, 2003]. The sampler was placed on the roof of a building belonging to the Xianghe Atmospheric Observatory of the Institute of Atmospheric Physics, Chinese Academy of Sciences, at a height of about 15 m above ground, from March to August 2005.

[10] During 12 h collection periods a manometer measured the pressure drop as the sampling flow-passed through an orifice plate. The recorded pressure drop was used to calculate the flow rate, which initially started at about 800 L/min upon filter change and dropped as the filter became loaded with particles. The total volume of air sampled by each filter ranged from 400 to 500 m^3 depending on the degree of aerosol loading. Exposed filters were stored frozen until initiation of observational and geochemical analyses.

2.2. Laboratory Analysis of Aerosols

[11] XRD, SEM, sulfate extractions, and isotopic analyses of the aerosol samples were conducted at the University of Maryland at College Park. For XRD analyses, small (1 × 1 cm) sections of selected filters were isolated and analyzed in the Chemistry Department X-ray Crystallography Facility. Samples on the filter squares were scanned with an X-ray analyzer to check for the presence of mineral particles, in

particular quartz (SiO_2) and gypsum ($CaSO_4$). Insofar as the filter paper itself has characteristic XRD peaks, clean sections of the filters were measured and the resulting peaks subtracted from the spectrum of peaks seen in scans of the samples. SEM observations of a representative sample were made in the Engineering Department SEM Facility.

[12] For extractions of soluble sulfate, sample filters were shredded and soaked overnight in 300 mL of Milli-Q (18 MΩ) water. Filters were isolated from solutions by centrifugation and the water-soluble sulfate was precipitated from solution as $BaSO_4$ by the addition of 3 mL of 1 mol/L $BaCl_2$ solution. After 30 min the precipitates were isolated from the solution by filtration through 0.22 μm acetate membrane discs. $BaSO_4$ particles on the filters were carefully rinsed with 150 mL Milli-Q water to remove Cl^- and were then transferred to ceramic crucibles and combusted at 800°C for one hour to quantitatively remove the acetate membrane filters and obtain high-purity $BaSO_4$.

[13] $BaSO_4$ was reduced to sulfide by gently boiling 25 mL of a reduction solution (HI + H_3PO_2 + HCl) [*Thode et al.*, 1961; *Forrest and Newman*, 1977] while purging with N_2, which carries sulfide through a water-cooled condenser and a water trap filled with Milli-Q water to remove chloride. Sulfide is chemically trapped as Ag_2S in a second trap filled with 15 mL of Milli-Q water, 1 mL of a 0.3 mol/L $AgNO_3$, and 2 mL of 1.55 mol/L HNO_3. The solution with precipitated Ag_2S was aged in the dark for 7 days, then filtered and rinsed with ~250 mL of Mill-Q water and ~5 mL of 1 mol/L NH_4OH. The Ag_2S precipitate was collected and transferred to an aluminum packet and dried in the oven for ~48 h.

2.3. Isotopic Analysis of Sulfur Isotopes

[14] Packages of aluminum foil containing ~3 mg of Ag_2S were loaded into nickel metal vessels, which were subsequently filled with fluorine gas and heated at ~300°C overnight to produce sulfur hexafluoride (SF_6). The SF_6 gas was purified using cryogenic distillation in a cold trap at −110°C to −115°C and further purified through a gas chromatography system using two 4.8 m 1/8 in. OD columns in series, the first being Molecular Sieve 5A column and the second being a Haysep Q column. The helium flow rate was set at 20 mL/min. SF_6 gas exiting the columns was frozen into two glass traps and was subsequently transferred to a sample bellows of a dual inlet ThermoFinnigan MAT 253 mass spectrometer where purified SF_6 was measured as SF_5^+ (m/e of 127, 128, 129, and 131). Uncertainties associated with the analyses for $\delta^{34}S$, $\Delta^{33}S$ and $\Delta^{36}S$ are estimated on the basis of long-term (repeat) measurements of standard materials to be ~0.20‰, ~0.008‰ and ~0.16‰ (1σ), respectively. Long-term measurements of IAEA S-1 with this instrument yield average $\delta^{34}S = -0.3$‰, $\Delta^{33}S = 0.094$‰, and $\Delta^{36}S = -0.69$‰.

3. Results and Discussion

3.1. Identification of Sulfur Sources

[15] Airborne calcium sulfate over China has been attributed to wind blown (eolian) mineral dust (as sedimentary gypsum, usually found as $CaSO_4 \cdot 2H_2O$) or to atmospheric reactions of calcium oxides or carbonates with H_2SO_4 [*Quan et al.*, 2008; *Takahashi et al.*, 2008]. But in a heavily populated and industrialized region such as Beijing, coal combustion seems a likely source. To determine the origin of sulfate aerosol, we conducted XRD analyses of five different samples. These revealed the presence of only quartz and gypsum as significant peaks, but the source of the gypsum remained a mystery. To further investigate the morphology of the gypsum grains, the same samples used in the XRD were imaged at high magnification with a SEM (Figures 1 and 2) and compared against SEM images from fly ash collected from a coal burning plant in western Maryland.

[16] The coal fly ash, which is typically filtered from smoke stack emissions, is primarily composed of euhedral crystals (Figure 1) and globular melt droplets of gypsum (Figure 2) determined by electron probe microanalysis (EPMX) using a JEOL 8900 Superprobe. These most likely form during reaction of SO_2, released during the combustion of abundant pyrite (FeS_2) in the coal, with Ca released from $CaCO_3$ minerals, which are also typically found in coal deposits. The euhedral morphology of the coal-derived gypsum grains is notably different from the rounded and pitted grains expected from gypsum dust transported by eolian (wind-blown) processes. The close comparison of the gypsum grains on the filter papers from this study with those from coal-fired fly ash suggests a previously underestimated source of primary sulfate to the atmosphere. Figures 1c–1h and 2c–2h show a variety of particles adhered to a representative filter from this study including euhedral laths, rosettes, and aggregates along with melt droplets of gypsum in a virtual sea of micron-sized spherical soot particles.

[17] The ubiquitous presence of soot particles as globular aggregates (Figures 1c and 1d and 2c and 2d) and chains (Figures 1h and 2h) adhered to the gypsum surfaces would intensify absorption of solar radiation and attenuate the single scattering albedo of these primary sulfate particles. These images may help illustrate the cause the unusually strong absorption of solar radiation by Asian aerosols, especially the absorption of the coarse mode [e.g., *Chaudhry et al.*, 2007; *Chaudhry*, 2008] (for methods see *Martins et al.* [2009]). This may be an important consideration in energy balance models of the atmosphere as discussed in section 1.

[18] The sulfur isotope data of Xianghe aerosols are presented in Table 1. The $\delta^{34}S$ values in Xianghe aerosols during the whole sampling period are within the range of 1.36 to 9.16‰ (Figure 3). The $\delta^{34}S$ values of aerosols during early spring range from 4.77‰ to 6.32‰ with an average and standard deviation of 5.35 ± 0.52‰ (1σ, n = 8), except for 1 March when a maximum value of 9.16‰ was reached. The $\delta^{34}S$ values of summer aerosols are more scattered with an average and standard deviation of 5.55 ± 2.13‰ (1σ, n = 18).

[19] Figure 4 describes the dependence of $\delta^{34}S$ values on sulfate concentrations in Xianghe aerosols. Sulfate concentrations in summer aerosols are much higher compared to those in spring aerosols with averages of 0.045 and 0.0092 mg/m^3, respectively. We note that $\delta^{34}S$ values and sulfate concentrations in early spring aerosols (open symbols) define a small range with the exception of the sample collected on 1 March. With the exception of this sample $\delta^{34}S$ values are observed to generally increase within a narrow window of increasing sulfate concentrations. This suggests that aerosol sulfates at the Xianghe site during early spring arise from simple sulfur sources. In contrast,

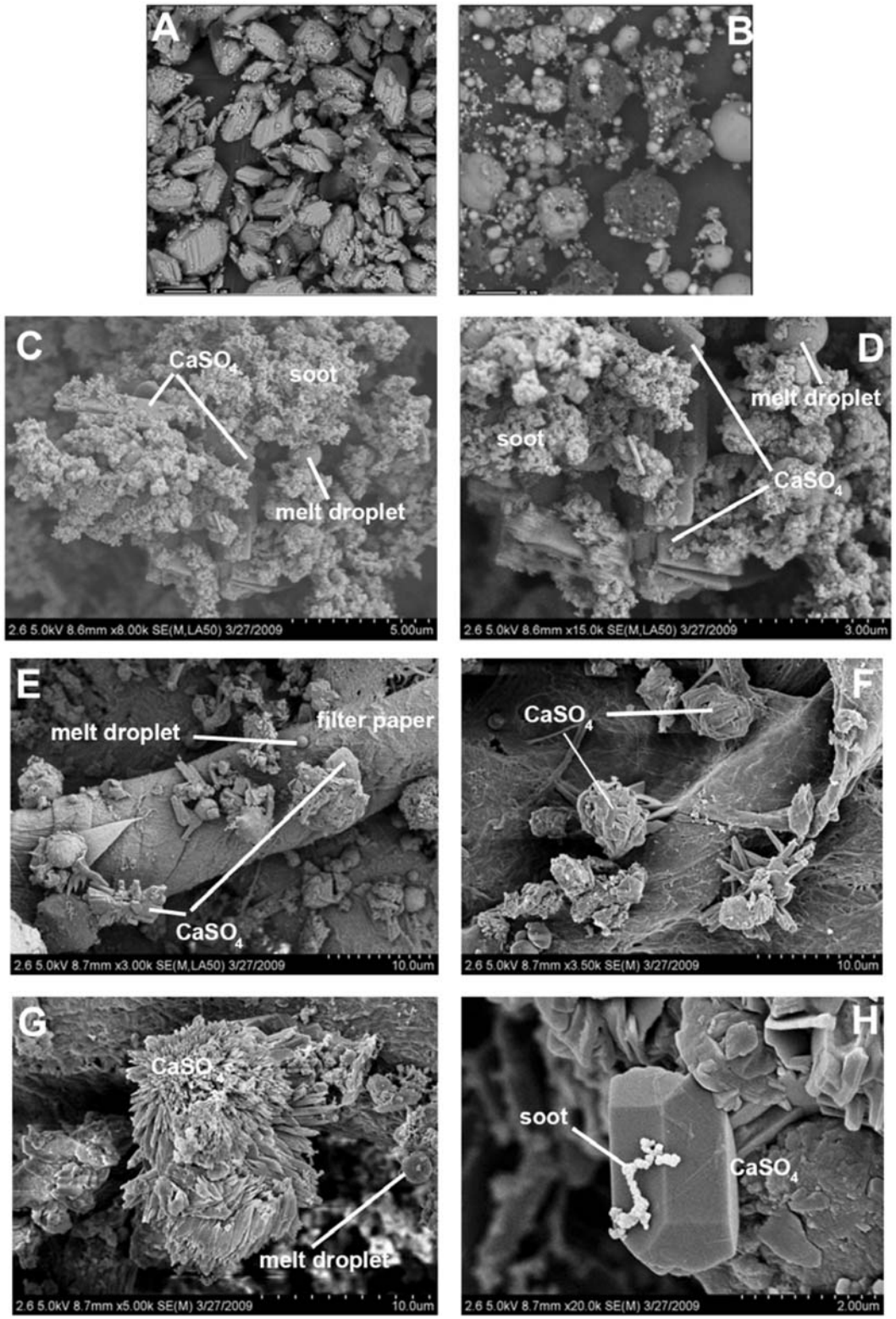

Figure 1. Positive photographs of SEM. (a) Euhedral gypsum crystals from fly ash collected from a coal-fired plant in western Maryland: scale is 50 μm. (b) Globular melt droplets of gypsum from same source: scale is 20 μm. (c) Euhedral laths and melt droplets of gypsum with aggregates of micron-sized soot particles: scale interval is 5 μm. (d) Closer view of 1C: scale interval is 3 μm. (e) Gypsum rosettes and melt droplets against filter paper: scale interval is 10 μm. (f, g) Large gypsum rosettes and aggregates: scale interval is 10 μm. (h) Euhedral gypsum crystal with chain of soot particles on surface: scale interval is 2 μm.

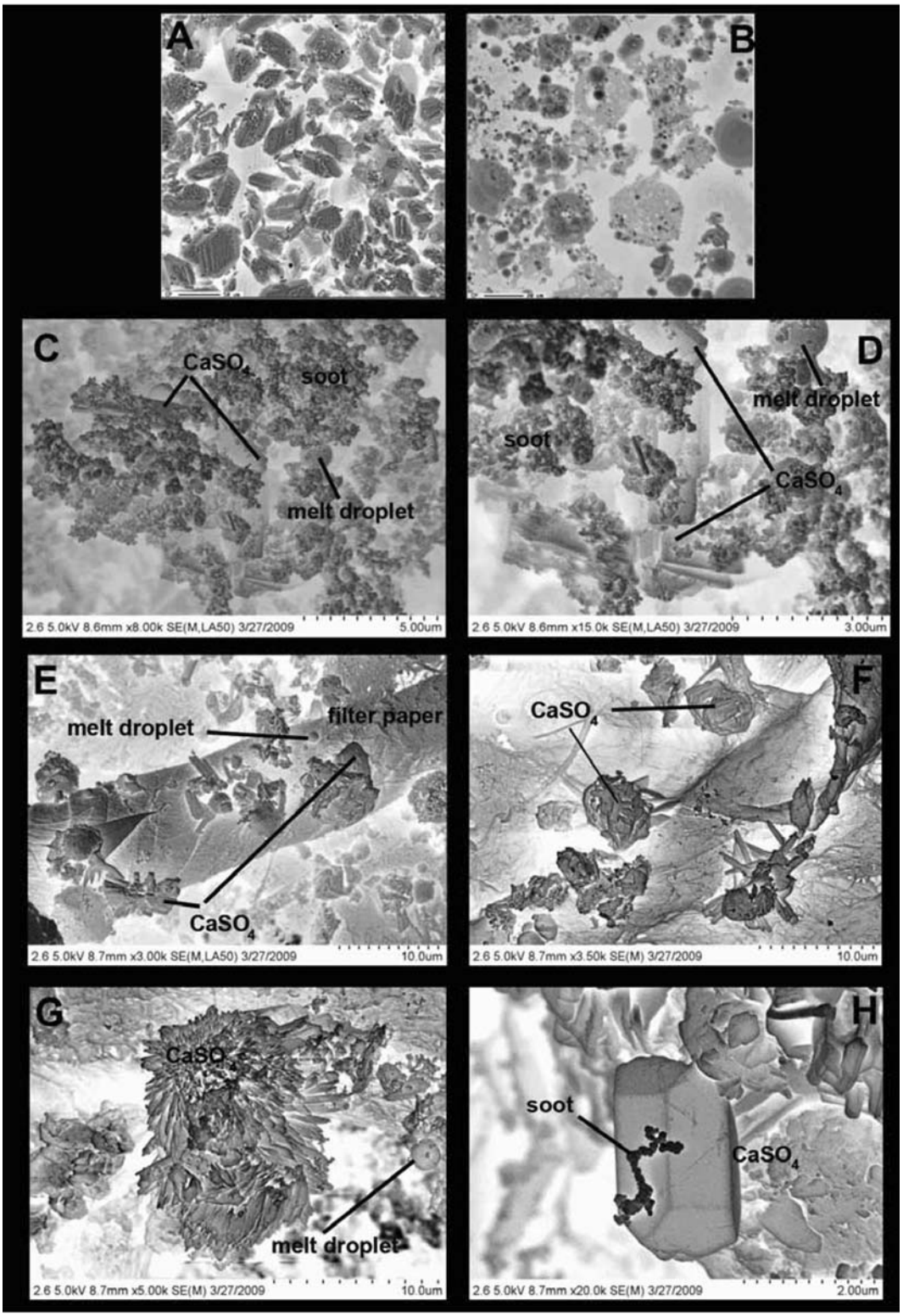

Figure 2. Same as Figure 1 but for negative (enhanced appearance for soot particles) photographs of SEM.

δ^{34}S values and sulfate concentrations in summer aerosols are more scattered, suggesting multiple sulfur sources and/or sulfate formation processes. Coal is a main energy source in China. It is reported that the average δ^{34}S value of coal used in northern China is ~4 to 5‰ [*Hong et al.*, 1992; *Mukai et al.*, 2001]. There exists a distinct sulfur isotope fractionation effect during coal combustion [*Zhang et al.*, 2002]. Compared to the δ^{34}S value of coal, the δ^{34}S values of SO_2 and solid particles produced from coal combustion in stoves decrease and increase, respectively [*Hong et al.*,

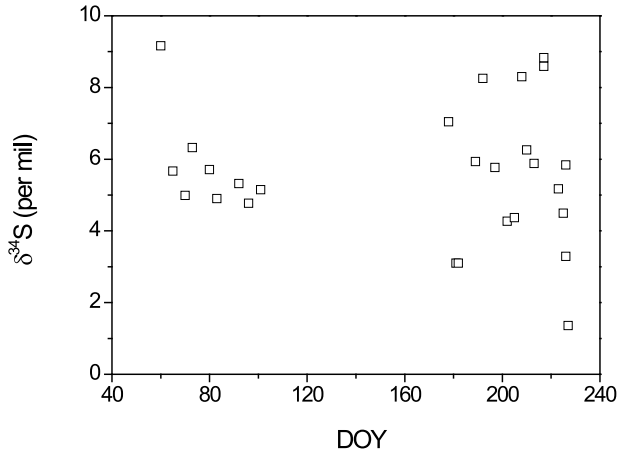

Figure 3. Time series of $\delta^{34}S$ values in Xianghe aerosols from March to August 2005. DOY stands for "day of year."

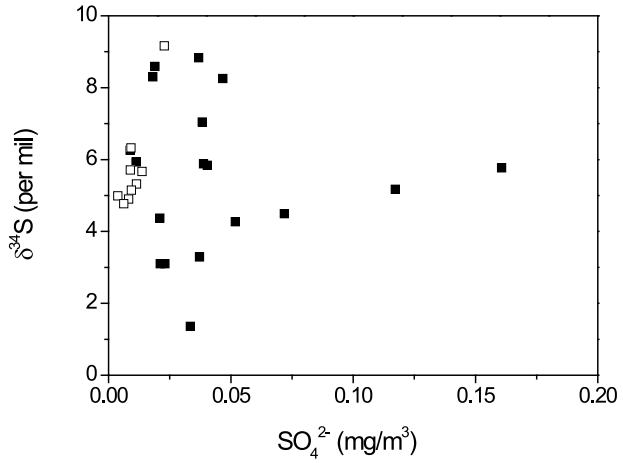

Figure 4. Dependence of $\delta^{34}S$ values on sulfate concentrations in Xianghe aerosols. Open squares represent spring aerosols, and solid squares stand for summer aerosols. Sulfate concentrations are from daylight averages.

1992; *Zhang et al.*, 2002]. For instance, the $\delta^{34}S$ value of SO_2 from coal combustion in the Pearl River Delta in southern China decreases by ~5‰ and the $\delta^{34}S$ value of solid particles increases by ~2.5‰ [*Zhang et al.*, 2002]. It is noteworthy that the average value of $\delta^{34}S$ in spring aerosol (~5.35‰) is close to that of particles emitted (~6‰) from coal combustion in northern China. Considering the common usages of high-sulfur coal combustion in factories over a wide area around the sampling site and the lack of strong SO_2 oxidation reactions due to cold and dry weather and weak solar radiation during early spring [*C. Li et al.*, 2007], we believe that a substantial fraction of springtime aerosol sulfates are primary sulfate particles mainly from direct emissions during coal combustion.

Table 1. Sulfur Isotope Data for Xianghe Aerosol Sulfate in 2005

Sampling Date	Day of Year	Sulfate Loading (mg/m^3)	$\delta^{34}S$(‰)	$\Delta^{33}S$(‰)	$\Delta^{36}S$(‰)
1 Mar	60	0.0248	9.16	0.040	−0.558
6 Mar	65	0.01474	5.67	−0.014	−0.725
11 Mar	70	0.00379	4.99	0.008	−0.356
14 Mar	73	0.00924	6.32	0.198	−0.839
21 Mar	80	0.00894	5.71	−0.056	−0.661
24 Mar	83	0.00824	4.90	0.129	−0.649
2 Apr	92	0.01143	5.32	0.126	−0.498
6 Apr	96	0.00623	4.77	0.047	−0.633
11 Apr	101	0.00934	5.15	0.233	−1.069
27 Jun	178	0.03832	7.04	0.194	−0.458
30 Jun	181	0.02305	3.10	0.241	−1.068
1 Jul	182	0.02115	3.10	0.151	−0.513
8 Jul	189	0.01131	5.93	0.200	−0.658
11 Jul	192	0.04674	8.25	0.157	−0.364
16 Jul	197	0.16074	5.77	0.069	−0.291
21 Jul	202	0.0519	4.27	0.302	−0.826
24 Jul	205	0.02098	4.37	0.207	−0.585
27 Jul	208	0.01815	8.30	0.180	−0.407
29 Jul	210	0.00885	6.26	0.184	−0.954
1 Aug	213	0.03886	5.88	0.119	−0.506
5 Aug	217	0.02601	8.59	0.216	−0.481
5 Aug	217	0.03183	8.83	0.290	−0.638
11 Aug	223	0.11728	5.17	0.142	−0.439
13 Aug	225	0.07187	4.49	0.459	−0.432
14 Aug	226	0.04038	3.29	0.478	−0.929
14 Aug	226	0.03717	5.84	0.525	−0.746
15 Aug	227	0.03351	1.36	0.434	−1.009

[20] Sulfuration processes also occur on the surface of most mineral particles, especially in summertime. Sulfuration is attributed to the absorption and coagulation of particles as well as reactions of absorbed SO_2 on particles surface. The seasonal variation in the sulfuration process on particle surface is observed to be associated with meteorological conditions at sampling sites [*Wen et al.*, 2007]. The higher temperature, relative humidity and O_3 concentration in summer leads to the stronger sulfuration and the more secondary sulfates on aerosols surface. This is a direction for further study to make clear whether and how analogous reactions through absorption and coagulation of particles are relevant in the atmosphere where sulfur gases are adsorbed on particle surfaces [e.g., *He et al.*, 2004; *Guo et al.*, 2007], and this may also be a significant contribution to the sulfate in the aerosols.

[21] A ground-based intensive observation campaign was held at the Xianghe site in March 2005, and in situ measurements of aerosol chemical compositions and trace gases were conducted (Figure 5). A good correlation exists among aerosol sulfate, CO and SO_2 concentrations in March 2005, indicating the presence of similar emission sources. Coal from northern China possesses an average sulfur content of 1.1–1.2% by weight and a maximum at 3% [*He and Chen*, 2002]. Low-efficiency stoves burning sulfur-containing coal emit CO and SO_2, as well as primary sulfates. Industrial and institutional boilers for heating are common in this part of China [*C. Li et al.*, 2007]. This supports the argument that aerosol sulfates at Xianghe during early spring are mainly from direct emission during coal combustion. According to data in Figure 5, the fraction of sulfur emitted as primary sulfate during coal combustion ranges from 10% to 45%.

[22] Figure 3 shows that the $\delta^{34}S$ value on 1 March (DOY = 60) was as high as 9.16‰, far higher than those seen in other springtime sulfates. Three day backward trajectories calculated every 6 h at 150 m above ground level on each sampling day (from the NOAA HYSPLIT model) and records of meteorological conditions were used to identify the sulfate sources on that day. Although the trajectories passed over the

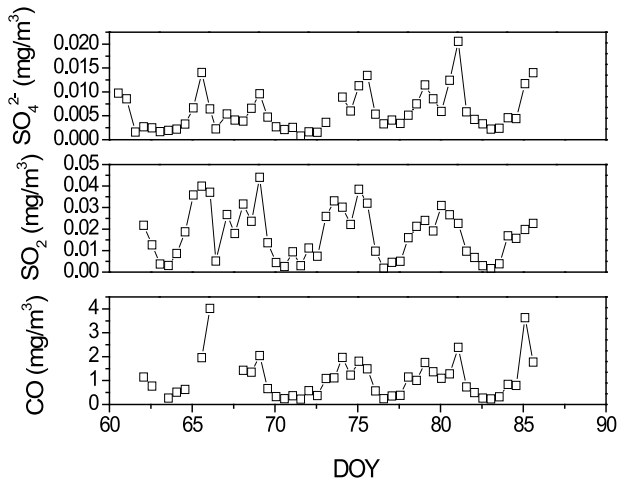

Figure 5. Concentrations of CO, SO_2, and sulfates observed at Xianghe in March 2005. CO and SO_2 data are from *C. Li et al.* [2007]. DOY stands for "day of year."

Bohai Bay area to the southeast on February 28 (DOY = 59) before reaching our sampling site, the mixing of sea salt ($\delta^{34}S \sim 21‰$) with aerosol sulfates is unlikely given the low Na^+ and Cl^- concentrations measured in the sample. Figure 6 shows the meteorological data during the sampling period. We note that the relative humidity of the atmosphere on 1 March was the highest recorded during the springtime period (72%), which might facilitate the heterogeneous oxidation of SO_2 to sulfate. The $\delta^{34}S$ values may thus reflect the production of secondary aerosol sulfate in the atmosphere during SO_2 oxidation. The measured fractionation with respect to source SO_2 is about −9‰ for homogeneous oxidation [*Saltzman et al.*, 1983; *Tanaka et al.*, 1994] and up to +16.5‰ for heterogeneous oxidation [*Eriksen*, 1972a, 1972b]. Therefore, the high $\delta^{34}S$ value on 1 March is attributed to the heterogeneous oxidation of SO_2 emitted from coal combustion.

[23] The scatter of sulfur isotope data with an average value $\delta^{34}S$ of 5.55‰ in summertime aerosols indicates different sulfur sources and/or the presence of different formation processes of aerosol sulfates (Figure 4). Water-soluble sulfates in aerosols may originate from both primary (eolian gypsum dust and, as shown here, particulate gypsum from coal combustion) and secondary sulfates. The oxidation of sulfur gases emitted from industrial, agricultural and biological activities are mainly responsible for the creation of secondary sulfates [*Bao and Reheis*, 2003]. Meteorological factors also have considerable influence over the sulfur isotope composition in aerosols via the effect on sulfate formation processes. In addition, rapid transport of SO_4^{2-} from regions having different $\delta^{34}S$ values may cause large fluctuations in sulfur isotope composition.

[24] Meteorological data (see Figure 6) illustrate the change from spring when average springtime air temperature is ~275 K and solar flux is 774 W/m^2 to summer when the average air temperature increases to ~299 K and solar flux increases to 965 W/m^2. These changes yield more conducive summer conditions for photochemical reactions and the production of oxidants (O_3, OH, and H_2O_2) in the troposphere. The O_3 concentration in Xianghe at the end of June was more than twice that at the end of March in 2005 [*Ma et al.*, 2007]. The high concentration of oxidants drives oxidation from SO_2 to sulfate, and is part of the reason why sulfate loading during summertime is much higher than that in springtime. Most of the annual rain in northern China falls in the summer monsoon season and the average relative humidity of the atmosphere during the summertime was ~73.5%, much higher than that during the springtime (~39%). Figure 6 also illustrates that sulfate concentrations in summertime aerosols are fairly well correlated with the relative humidity of the atmosphere. Therefore, these meteorological data in summer are observed to be favorable for heterogeneous oxidation of SO_2.

[25] As mentioned earlier, $\delta^{34}S$ values may change if SO_2 is oxidized into secondary aerosol sulfates in the atmosphere via different homogeneous and heterogeneous reactions. The $\delta^{34}S$ compositions of precursor SO_2 can be predicted with knowledge of the $\delta^{34}S$ value of secondary sulfate and SO_2 oxidation pathways [*Winterholler et al.*, 2008]. Assuming 50% of the summer aerosol sulfates are produced via heterogeneous oxidation and another half by homogenous oxidation of SO_2, the increase in $\delta^{34}S$ value of summer aerosol sulfates should be ~3.75‰, and the actual $\delta^{34}S$ value increase is expected to be >3.75‰ due to the dominant heterogeneous oxidation of SO_2 in summer sulfate formation. Considering the average $\delta^{34}S$ value in summer aerosol sulfate of ~5.55‰, precursor SO_2 with $\delta^{34}S$ value lower than 1.8‰ must be present. This is broadly consistent with the range of $\delta^{34}S$ values of SO_2 from coal combustion. It should be noted that the $\delta^{34}S$ signature of biogenic sulfur emitted from anoxic surface environments to the atmosphere is less than 0‰. Thus, biogenic sulfur associated with higher soil moisture is a possible strong source of summer sulfate particles, especially for aerosol samples with low $\delta^{34}S$. For example, *Zhang et al.* [2002] measured sulfur isotope compositions of acid deposition in Pearl River Delta and found the contribution rate of biogenic sulfur reached 52% in June 1996.

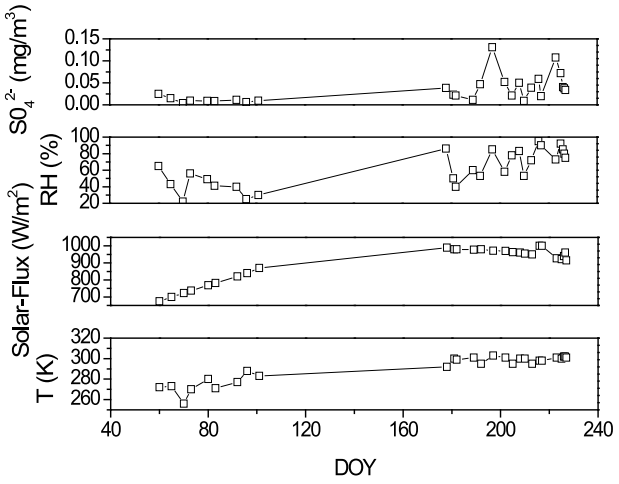

Figure 6. Air temperature (T, K), solar flux (W/m^2), relative humidity (RH, %) at 0600 GMT each day, and daylight averaged sulfate concentration (mg/m^3) at the Xianghe site from March to August 2005. DOY stands for "day of year."

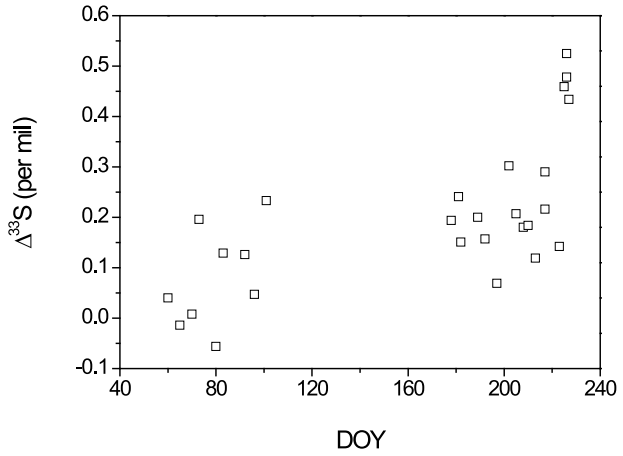

Figure 7. Time series of $\Delta^{33}S$ values in Xianghe aerosols from March to August 2005. DOY stands for "day of year."

3.2. Sulfur Isotope Anomalies

[26] Figure 7 shows the time series of $\Delta^{33}S$ values in aerosol sulfates. $\Delta^{33}S$ values generally increase from spring to summer. $\Delta^{33}S$ values for early March aerosols are close to 0‰ while those in April are slightly higher, with a maximum $\Delta^{33}S$ value of 0.233‰ on 11 April (last sampling day in April, DOY = 101). During the summer sampling period (June to August) the average $\Delta^{33}S$ value is even higher (0.253‰). $\Delta^{33}S$ values of aerosols from 13–15 August (DOY = 225–227) range from 0.434 to 0.525‰. The mean and median $\Delta^{33}S$ values for the whole sampling period are 0.192‰ and 0.182‰, respectively.

[27] When $|\Delta^{33}S| \leq 0.1‰$ it can be difficult to tell whether a mass-independent signal exists or not, but when $|\Delta^{33}S| \geq 0.1‰$ and the $\delta^{34}S$ values do not vary by more than about 10‰, it is possible to argue for the presence of a mass-independent effect. (Photopolymerization of carbon disulfide also does not make sense in this case because only water-soluble sulfates were analyzed in our study as well as low concentrations and slow photopolymerization reactions for CS and CS_2, their contributions on mass-independent sulfur isotope compositions in aerosols are negligible.) Using this reasoning, the $\Delta^{33}S$ values from samples taken from middle March to August, those are generally higher than 0.1‰, likely reflect a mass-independent sulfur isotope fractionation process.

[28] As indicated in Figure 8, $\Delta^{33}S$ and $\delta^{34}S$ values in Xianghe aerosols have a similar range with those in submicron aerosols from La Jolla, California [*Romero and Thiemens*, 2003]. In addition, the scatter in the $\Delta^{33}S$ and $\delta^{34}S$ data suggests multiple sources that likely include a combination of mass-dependent and mass-independent processes. It is observed that $\delta^{34}S$ values do not converge at high values of $\Delta^{33}S$ (0.434‰ to 0.525‰), which suggests that the mass-independent effect either involved mixing of two distinct mass-independent components, or a single mass-independent component that was subsequently processed by a mass-dependent reaction. Meanwhile, we also note the nonconvergence of $\delta^{34}S$ values at relatively low $\Delta^{33}S$ values (0.119‰ to 0.302‰). The general increase in $\delta^{34}S$ values and decrease in $\Delta^{33}S$ values indicate the mixing between a high $\delta^{34}S$ mass-dependent component and a mass-independent component with the low $\delta^{34}S$ value. On the other hand, $\delta^{34}S$ values also scatter at the $\Delta^{33}S$ value of 0‰, which implies a second mass-dependent end-member. As mentioned earlier, aqueous heterogeneous (in cloud) oxidation of SO_2 in early spring is a viable alternative end-member.

[29] In addition, negative $\Delta^{36}S$ values are observed independent of the sampling time. $\Delta^{36}S$ values vary from −1.069‰ to −0.291‰, most of which are more negative than −0.4‰. It should be emphasized that there is the presence of the negative correlation between $\Delta^{33}S$ and $\Delta^{36}S$ values especially in summer aerosols (Figure 9).

3.3. Mechanisms for Producing Mass-Independent Sulfur Isotope Anomalies

[30] The mechanisms related to mass-independent sulfur isotope fractionation in present-day aerosol sulfates are not clear. Mass-independent isotopic compositions have been attributed to a variety of causes, including those that affect bonding directly and those that affect reaction rates for different isotopomers (kinetic isotope effects). Nuclear field shift effects can be classified as those that occur because of the way that the charge density of the nucleus affects the shape of the potential well that describes the chemical bonds involving different isotopes [e.g., *Bigeleisen*, 1998]. This class of effect exists because of a direct change in the chemical bonds for different isotopomers. This effect would be relevant in exchange reactions, but in the case of light elements like sulfur it is not thought to be significant, and is therefore not considered as a candidate for our observations.

[31] Kinetic isotope effects (KIE) are related to reaction rate enhancements for some isotopomers. KIE that have been suggested to be mass-independent include those associated with surface reaction effects [*Lasaga et al.*, 2008], spin coupling (magnetic isotope effects (MIE)) [*Buchachenko*, 2000], symmetry [*Gao and Marcus*, 2001], self-shielding [e.g., *Lyons* 2008], or chance vibronic overlap of excited

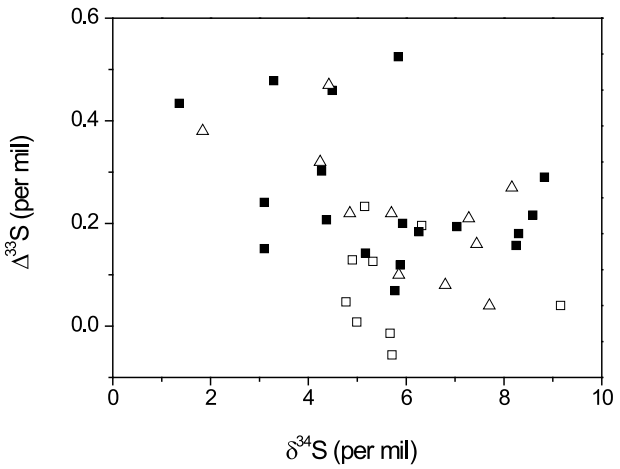

Figure 8. $\Delta^{33}S$ as a function of $\delta^{34}S$ in Xianghe aerosol from March to August 2005. Open squares represent spring aerosols, and solid squares represent summer aerosols. Open triangles are data from *Romero and Thiemens* [2003].

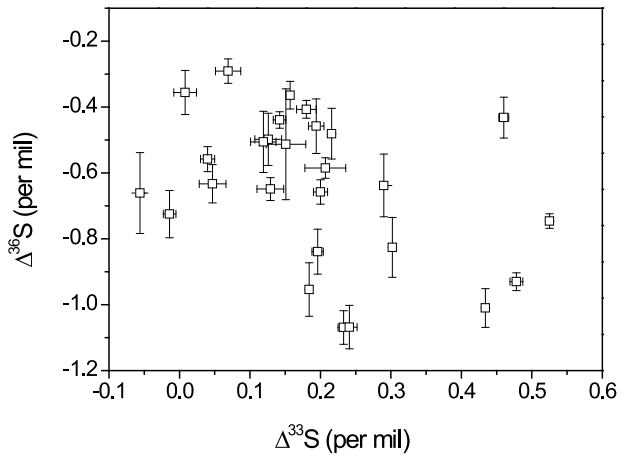

Figure 9. Relation between $\Delta^{36}S$ and $\Delta^{33}S$ in Xianghe aerosols from March to August 2005. Error bars represent estimates of the 2σ uncertainty.

states of different isotopomers [e.g., *Zmolek et al.*, 1999; *Romero and Thiemens*, 2003]. Of these, the surface reaction model of *Lasaga et al.* [2008] and the well-established MIE [*Buchachenko*, 2000] are the only reactions that would apply to heterogeneous reactions (MIE also to gas phase), but we suggest that it is possible to rule these out as viable candidates for our observations. There is presently no clear experimental evidence to support the reaction model of *Lasaga et al.* [2008] and there is also discussion in the literature [e.g., *Balan et al.*, 2009] that disputes this mechanism. MIE cannot explain the relationships for $\Delta^{36}S$. The remaining homogeneous pathways may also have weaknesses. For instance, symmetry may not be a reasonable candidate in this case because the sulfur atoms occupy a central position in the gaseous S(IV) precursors to S(VI). Self shielding may or may not be important in today's atmosphere because many of the S(VI) oxidation pathways involve species produced through photochemistry such as OH and H_2O_2, but are not photolytic, that is SO_2 itself is not photolyzed, although absorption of solar UV photons leads excitation. Reactions involving electronically excited SO_2 (1A2 or 1B1) have long been thought unimportant in the lower troposphere because of rapid quenching [*Calvert et al.*, 1978], but in the upper troposphere the UV flux is enhanced and quenching is an order of magnitude slower. The same may apply to effects rooted in vibronic overlap. These effects have however been demonstrated in laboratory experiments with sulfur gases such as SO_2, and these gas-phase effects have been invoked in prior studies that seek to explain mass-independent sulfur in aerosol samples. We therefore accept this as the most likely mechanism to explain our observations, but add the caveat that at present we do not fully understand the origin of the effects that we see.

[32] Other studies have suggested that photochemical reaction mechanisms are presently the leading candidate for the effect, and it is largely because this is one candidate for which large isotope anomalies in $\Delta^{33}S$ and $\Delta^{36}S$ have been produced [*Farquhar et al.*, 2001; *Romero and Thiemens*, 2003; *Ueno et al.*, 2008]. In itself this does not constitute proof that photochemical processes involving sulfur dioxide are the root of the observed mass-independent fractionation, but it does provide a mechanism that is possible and can be tested.

[33] Research done to date has been largely exploratory and includes studies of photolysis of SO_2 and H_2S [*Farquhar et al.*, 2000b, 2001] and photopolymerization of CS and CS_2 [*Colman et al.*, 1996; *Zmolek et al.*, 1999]. Photodissociation of H_2S can produce isotope anomalies in $\Delta^{33}S$ and $\Delta^{36}S$, and its products can be simultaneously depleted or enriched in either ^{33}S and ^{36}S [*Farquhar et al.*, 2000b], but there is a strong isotope effect expressed in $\delta^{34}S$ as well, which is not seen in the aerosol samples taken from Xianghe. The same issue is present for photopolymerization of CS_2^i and for photolysis of sulfur dioxide with continuum radiation longer than ~220 nm. *Danielache et al.* [2008] reported measurements of the ultraviolet absorption cross sections of $^{32}SO_2$, $^{33}SO_2$, and $^{34}SO_2$, and argued that large wavelength-dependent and broadband isotopic fractionations were related to UV photolysis of SO_2. Shorter wavelength photolysis (<220 nm) appears to produce significant isotope anomalies in $\Delta^{33}S$ and $\Delta^{36}S$ without producing significant effects in $\delta^{34}S$. It is these latter reactions that have been called upon by previous studies [*Romero and Thiemens*, 2003; *Savarino et al.*, 2003; *Baroni et al.*, 2007] and the requirement of short wavelengths has cited the reactions that produce the effects in the stratosphere. Note that the reactions that produce the effect may be related to sulfur dioxide, or they may be related to photolysis of long-lived bound states (or intermediates) [*Farquhar et al.*, 2001; *Lyons*, 2008]. The intensity of UV radiation at these wavelengths in the troposphere is too low to play a significant role in SO_2 dissociation there.

[34] It is difficult to directly ascribe the data for the aerosol measurements to any existing photochemical experimental results. Some features of the data are broadly consistent with other observations that have been attributed to photochemical effects (e.g., the possible negative correlation between $\Delta^{33}S$ and negative $\Delta^{36}S$ values (see Figure 9), but other features of the data are more difficult to match with the experiments (e.g., the lack of a clear ^{34}S signal combined with the sign of the $\Delta^{33}S$ and negative $\Delta^{36}S$ signals in the product sulfate). The experimental and theoretical constraints on the fractionations are limited, however, and attribution of the signal to a specific photochemical effect (or effects) remains to be demonstrated. There is also a possibility that the isotopic characteristics may reflect a combination of mass-dependent effects, mass-independent effects, and preexisting signals inherited from the sulfur in the coal used for combustion. For instance, the $\delta^{34}S$ value of sulfur in coal from northern China (~4 to 5‰ [*Hong et al.*, 1992; *Mukai et al.*, 2001]) is nonzero and the $\Delta^{36}S$ may be nonzero as well because ^{36}S depletions and enrichments relative to the reference fractionation array have been observed in biological processing [*Johnston et al.*, 2007]. It is possible (but not a forgone conclusion) that the sulfur isotope variations in the aerosol samples taken from Xianghe represent mixing of a component with mass-independent $\Delta^{33}S$ and $\Delta^{36}S$ values with another component that has an inherited negative $\Delta^{36}S$, ultimately derived from anthropogenic or biological sources.

[35] Other possibilities may exist. These include the view that the anomalous $\Delta^{33}S$ derived ultimately from anthropogenic emissions may tap sulfur that had positive $\Delta^{33}S$

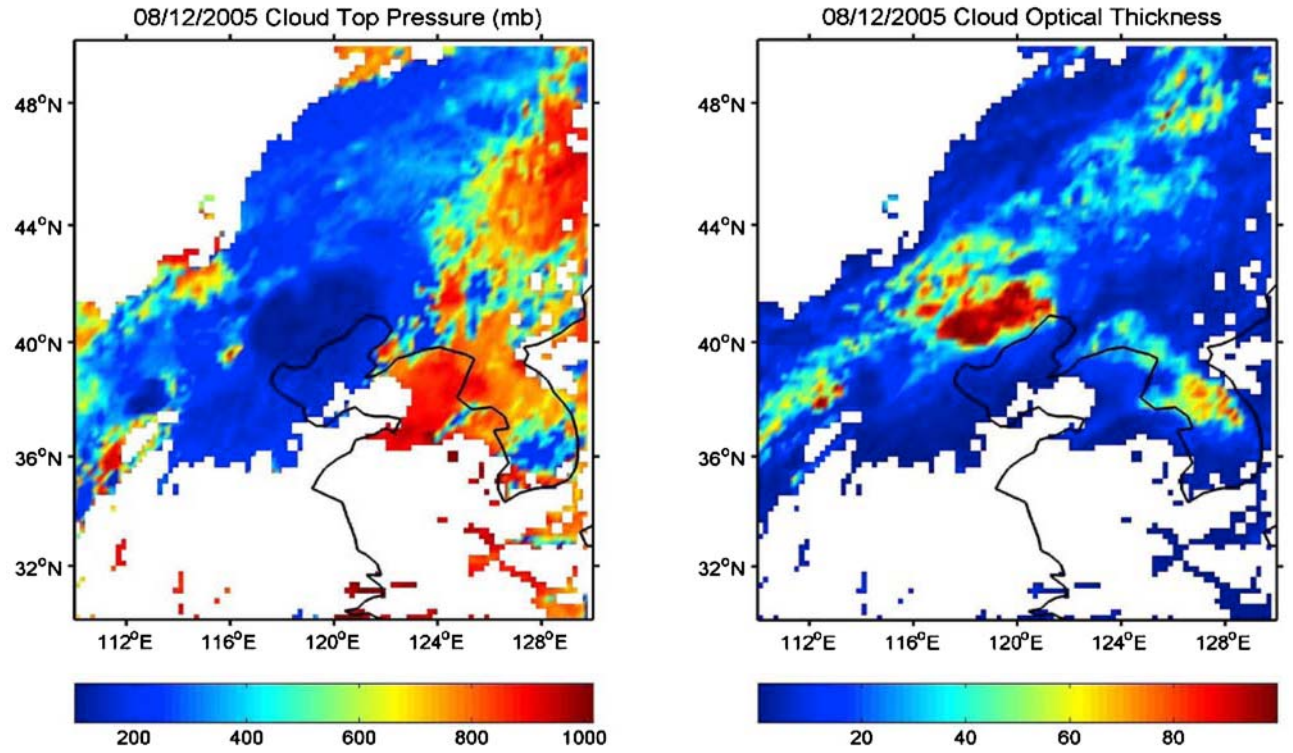

Figure 10. Evidences of the presence of deep convection events around Xianghe site starting from 12 August 2005 based on satellite data of (left) cloud top pressure and (right) cloud optical depth.

such as may be the case with smelting of ancient (Archean age) iron ores that possess nonzero $\Delta^{33}S$. Note that a relationship of $\Delta^{33}S \sim -\Delta^{36}S$ has been observed for rocks of this age [*Farquhar et al.*, 2000a; *Farquhar and Wing*, 2003] but exceptions have been observed [*Farquhar et al.*, 2007] which would allow for this possibility. Other pathways such as oxidation of SO_2 or DMS (dimethylsulfide) from the environment in the gas phase by OH radicals are presently not considered to be a source for mass-independent sulfur isotope fractionation [*Romero and Thiemens*, 2003; *Bao et al.*, 2000]. SO_3 photolysis has also been proposed to as a possible source for mass-independent sulfur isotope fractionation based on results from the Garcia-Solomon 2-D dynamical/chemical model with aerosol microphysics [*Pavlov et al.*, 2005]. *Baroni et al.* [2007] regarded this as a minor process for producing a large amount of sulfate due to the fast reaction between SO_3 and H_2O in today's atmosphere. It appears therefore that the origin of the mass-independent signature in the aerosol samples taken from Xianghe either represent stratospheric input or some other not-yet-identified tropospheric processes.

3.4. Relationship of Convective Processes and $\Delta^{33}S$ Anomalies

[36] In our study, $\Delta^{33}S$ values in aerosols on 13, 14 (day and night), and 15 August are 0.460, 0.525, 0.478 and 0.434‰, respectively, which are much higher than those of aerosols collected at other times during the sampling period, leading us to investigate further the possibility that they preserve information about the origin of the sulfur isotope anomaly.

[37] During this interval, deep convective clouds are seen over the area on 12 August in satellite data. Low cloud top pressures and high cloud optical thicknesses over a large area around the sampling site on 12 August are illustrated in Figure 10. Thunderstorms were also observed on 13 and 15 August at the Xianghe site. This evidence supports the hypothesis that the sulfur isotope anomalies may be related to a deep convection processes active in the region at the time. Another measure of convection is given by CAPE (Convective Available Potential Energy) which is widely used to measure atmospheric instability and is also used to predict severe weather, and to determine how powerful those storms might become if they do occur [*Demott and Randall*, 2004]. In general, CAPE values in excess of 2500 J/kg indicate that the atmosphere could supply ample energy for strong updrafts and violent storms should develop. According to sounding data from the Beijing observation station for the time period covered in this study (see Figure 11; 13–15 August) about 12 h before the sampling time, CAPE values as high as 2096, 3768, 2743 and 2486 J/kg were recorded. This indicates the presence of a severe air mass convective process under extreme local weather conditions, which is favorable for the exchange of the lower tropospheric and upper tropospheric or even stratospheric air. *Oltmans and Hofmann* [1995] observed the existence of additional natural sources of H_2O in the low stratosphere from moist convection during the summer months. *Dickerson et al.* [1987] and *Poulida et al.* [1996] suggested that thunderstorms, with strong convective processes, were one means of rapid transport of pollutants from the lower troposphere to the upper tropopause and low

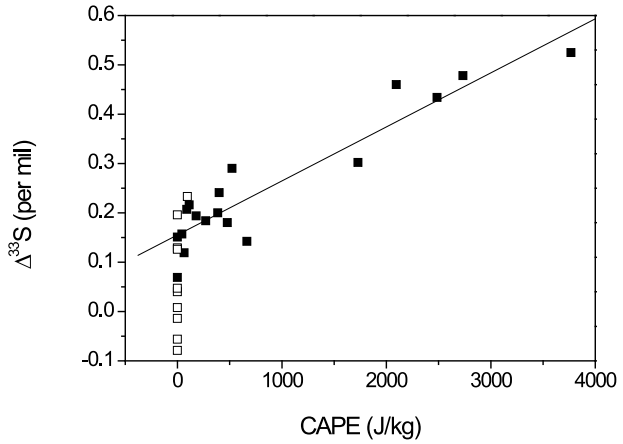

Figure 11. The dependence of Δ^{33}S values on CAPE values in spring and summer aerosols sampled from Xianghe. CAPE values were measured at ~12 h before the sampling time. Open squares represent spring aerosols, and solid squares represent summer aerosols. The line is from linear regression for summer aerosols.

stratosphere via the anvil and overshooting tops. *Tanaka and Turekian* [1995] observed cosmogenically produced radionuclides ^{35}S and ^{7}Be in summer aerosols on the east coast of United States, suggesting large stratospheric outputs of sulfate to near ground level. The transport of aerosol sulfates and gases in the lower stratosphere and upper tropopause into the lower troposphere also takes place in the downdrafts of backward anvils [*Stenchikov et al.*, 1996].

[38] Considering CAPE values on the three days in August that are significantly large, we suggest that the large Δ^{33}S values in these aerosol sulfate are associated with violent convective processes. These generate strong updrafts and overshooting tops or anvils that could reach the tropopause and low stratosphere, thereby facilitating sulfate transport from low stratosphere and upper troposphere to near ground level resulting in larger sulfur isotope anomalies in these populations of aerosols. Figure 11 illustrates a possible dependence of Δ^{33}S values on CAPE values in spring and summer aerosols sampled from Xianghe (e.g., in summer, $R = 0.933$, $P < 0.0001$). Figure 11 also shows that some Δ^{33}S values are greater than 0.1‰ despite CAPE values at 0 J/kg. The variation in sulfur isotopes is hard to interpret using only stratospheric photochemical reactions of SO_2. The presence of Δ^{33}S values greater than 0.1 for aerosol samples from June and July, as well as for some samples collected earlier in the season may reflect less intense atmospheric mixing, or they may reflect a lower tropospheric process associated with sulfate formation that also generates mass-independent fractionations. Thus it appears that sulfur isotope anomalies in aerosol samples gathered at Xianghe are related to other mechanisms.

[39] Generally speaking, the March samples should also carry a signature of mixing of lower stratospheric or upper tropospheric air masses in the Northern Hemisphere [*Lee*, 2000], and limited evidence for this exists. However, Δ^{33}S values measured from samples of aerosol sulfates in March are generally lower than those from other sampling times. The reason for this observation is not clear, but it is suggested to be related to sources of sulfate coming predominantly from coal burning accompanied by less intense atmospheric mixing and less intense atmospheric oxidation.

4. Conclusions

[40] In this paper we evaluated the source of atmospheric aerosols at a rural site in northern China (Xianghe, 39.75°N, 116.96°E) from March to August 2005 by detailed observations of filtered particles and isotopic investigations of calcium sulfate. The SEM observations of filter papers reveal a novel primary source of sulfate to the atmosphere through coal combustion. This may be an important factor in calculations of the radiative balance of the atmosphere, due to the cooccurrence of reflective gypsum particles and of absorptive soot attached to these particles. We attribute sulfur in early spring aerosols to direct emissions of sulfate particles during coal combustion due to their equivalent δ^{34}S values and weak oxidation of SO_2. A ground-based intensive observation campaign was simultaneously carried out and the results supported our conclusions [*C. Li et al.*, 2007].

[41] The measured sulfur isotope abundances (^{32}S, ^{33}S, ^{34}S and ^{36}S) of soluble sulfate from these filters reveals (1) a relationship between Δ^{33}S and CAPE, measure atmospheric instability that suggests a high-altitude (stratosphere or upper troposphere) source as well as (2) the presence of higher Δ^{33}S during summer, suggesting a more significant role for atmospheric oxidation pathways of SO_2 at this time. The origin of the mass-independent isotope effect remains unresolved and further studies are needed to identify these effects and to determine whether they can be used to provide quantitative constraints on mixing of upper and lower atmospheric aerosol populations.

[42] **Acknowledgments.** The authors wish to thank Phil Piccoli in the Geology Department for providing images of coal fly ash from western Maryland, Peter Zavilij in the Chemistry Department for XRD analysis, Wen-an Cho in the Engineering Department for SEM/TEM analysis, Craig Hebert in the Geology Department for isotopic analyses, and W. Lan in the Institute of Atmospheric Physics for acquiring the filter papers. This research was supported by MOST (2006CB403706), NASA (NNG04GE79G), DOE (DEFG0208ER64571), Jiangsu Province National Science foundation (BK2009414), Qinglan project of Jiangsu Province, and a grant from NUIST (20080316). A Guggenhiem Fellowship (J.F.), a University of Maryland Graduate fellowship (N.P.W.), and the Danish National Science Foundation (J.F.) also support this research.

References

Balan, E., P. Cartigny, M. Blanchard, D. Cabaret, M. Lazzeri, and F. Mayri (2009), Erratum to "Theoretical investigation of the anomalous equilibrium fractionation of multiple sulfur isotopes during adsorption," *Earth Planet. Sci. Lett.*, *284*, 88–93, doi:10.1016/j.epsl.2009.04.010.

Bao, H. M., and M. C. Reheis (2003), Multiple oxygen and sulfur isotopic analyses on water-soluble sulfate in bulk atmospheric deposition from the southwestern United States, *J. Geophys. Res.*, *108*(D14), 4430, doi:10.1029/2002JD003022.

Bao, H., M. H. Thiemens, J. Farquhar, D. A. Campbell, and C. C. W. Lee (2000), Anomalous ^{17}O compositions in massive sulphate deposits on the Earth, *Nature*, *406*, 176–178, doi:10.1038/35018052.

Baroni, M., M. H. Thiemens, R. J. Delmas, and J. Savarino (2007), Mass-independent sulfur isotopic compositions in stratospheric volcanic eruptions, *Science*, *315*, 84–87, doi:10.1126/science.1131754.

Bigeleisen, J. (1998), Second-order correction to the Bigeleisen–Mayer equation due to the nuclear field shift, *Proc. Natl. Acad. Sci. U. S. A.*, *95*, 4808–4809, doi:10.1073/pnas.95.9.4808.

Buchachenko, A. L. (2000), Recent advances in spin chemistry, *Pure Appl. Chem.*, *72*(12), 2243–2258, doi:10.1351/pac200072122243.

Calvert, J. G., F. Su, J. W. Bottenheim, and O. P. Strausz (1978), Mechanism for the homogeneous oxidation of sulfur dioxide in the troposphere, *Atmos. Environ.*, *12*, 197–226, doi:10.1016/0004-6981(78)90201-9.

Chameides, W. L., et al. (1999), Case study of the effects of atmospheric aerosols and regional haze on agriculture: An opportunity to enhance crop yields in China through emission controls?, *Proc. Natl. Acad. Sci. U. S. A.*, *96*, 13,626–13,633, doi:10.1073/pnas.96.24.13626.

Chaudhry, Z. (2008), A study of optical, physical, and chemical properties of aerosols using in situ measurement, Ph.D. dissertation, Univ. of Md., College Park.

Chaudhry, Z., J. V. Martins, Z. Li, S. C. Tsay, H. Chen, P. Wang, T. Wen, C. Li, and R. R. Dickerson (2007), In situ measurements of aerosol mass concentration and radiative properties in Xianghe, southeast of Beijing, *J. Geophys. Res.*, *112*, D23S90, doi:10.1029/2007JD009055.

Cheng, Y. F., et al. (2009), Influence of soot mixing state on aerosol light absorption and single scattering albedo during air mass aging at a polluted regional site in northeastern China, *J. Geophys. Res.*, *114*, D00G10, doi:10.1029/2008JD010883.

Clarke, A. D., et al. (2004), Size distributions and mixtures of dust and black carbon aerosol in Asian outflow: Physiochemistry and optical properties, *J. Geophys. Res.*, *109*, D15S09, doi:10.1029/2003JD004378.

Colman, J. J., X. Xu, M. H. Thiemens, and W. C. Trogler (1996), Photopolymerization and mass-independent sulfur isotope fractionations in carbon disulfide, *Science*, *273*, 774–776, doi:10.1126/science.273.5276.774.

Danielache, S. O., C. Eskebjerg, M. S. Johnson, Y. Ueno, and N. Yoshida (2008), High-precision spectroscopy of ^{32}S, ^{33}S, and ^{34}S sulfur dioxide: Ultraviolet absorption cross sections and isotope effects, *J. Geophys. Res.*, *113*, D17314, doi:10.1029/2007JD009695.

Demott, C. A., and D. A. Randall (2004), Observed variations of tropical convective available potential energy, *J. Geophys. Res.*, *109*, D02102, doi:10.1029/2003JD003784.

Dickerson, R. R., et al. (1987), Thunderstorms: An important mechanism in the transport of air pollutants, *Science*, *235*, 460–464, doi:10.1126/science.235.4787.460.

Ding, T., S. Valkiers, H. Kipphardt, P. D. Bièvre, P. D. P. Taylor, R. Gonfiantini, and R. Krouse (2001), Calibrated sulfur isotope abundance ratios of three IAEA sulfur isotope reference materials and V–CDT with a reassessment of the atomic weight of sulfur, *Geochim. Cosmochim. Acta*, *65*(15), 2433–2437, doi:10.1016/S0016-7037(01)00611-1.

Eriksen, T. E. (1972a), Sulfur isotope-effects.1. Isotopic-exchange coefficient for sulfur isotopes $^{34}S^{-32}S^{-}$ in the system SO_2g-HSO_3-aq at 25, 35, and 45 degrees C, *Acta Chem. Scand.*, *26*, 573–580, doi:10.3891/acta.chem.scand.26-0573.

Eriksen, T. E. (1972b), Sulfur isotope-effects. 3. Enrichment of $^{34}S^{-}$ by chemical exchange between SO_2g and aqueous-solutions of SO_2, *Acta Chem. Scand.*, *26*, 975–979, doi:10.3891/acta.chem.scand.26-0975.

Farquhar, J., and B. A. Wing (2003), Multiple sulfur isotopes and the evolution of the atmosphere, *Earth Planet. Sci. Lett.*, *213*, 1–13, doi:10.1016/S0012-821X(03)00296-6.

Farquhar, J., et al. (2000a), Atmospheric influence of Earth's earliest sulfur cycle, *Science*, *289*, 756–758, doi:10.1126/science.289.5480.756.

Farquhar, J., J. Savarino, T. L. Jackson, and M. H. Thiemens (2000b), Evidence of atmospheric sulfur in the Martian regolith from sulphur isotopes in meteorites, *Nature*, *404*, 50–52, doi:10.1038/35003517.

Farquhar, J., J. Savarino, S. Airieau, and M. H. Thiemens (2001), Observation of wavelength-sensitive mass-independent sulfur isotope effects during SO_2 photolysis: Implications for the early atmosphere, *J. Geophys. Res.*, *106*(E12), 32,829–32,839, doi:10.1029/2000JE001437.

Farquhar, J., et al. (2007), Isotopic evidence for Mesoarchaean anoxia and changing atmospheric sulphur chemistry, *Nature*, *449*, 706–709, doi:10.1038/nature06202.

Forrest, J., and L. Newman (1977), Ag-110 microgram sulfate analysis for short time resolution of ambient levels of sulfur aerosol, *Anal. Chem.*, *49*, 1579–1584, doi:10.1021/ac50019a030.

Gao, Y. Q., and R. A. Marcus (2001), Strange and unconventional isotope effects in ozone formation, *Science*, *293*, 259–263, doi:10.1126/science.1058528.

Guo, X. Q., Y. F. Wang, Y. Z. Shi, X. R. Li, and Y. S. Wang (2007), Determination of organic acids in atmospheric aerosol during heating period in Beijing (in Chinese), *J. Instrum. Anal.*, *26*, 181–184.

He, B. S., and C. H. Chen (2002), Energy ecological efficiency of coal fired plant in China, *Energy Convers. Manage.*, *43*, 2553–2567, doi:10.1016/S0196-8904(01)00191-1.

He, L. Y., M. Hu, X. F. Huang, and Y. H. Zhang (2004), Determination of politary organic compounds in atmospheric fine particle matter in Beijing city (in Chinese), *Environ. Sci.*, *25*(5), 16–22.

Höller, R., K. Ito, S. Tohno, and M. Kasahara (2003), Wavelength-dependent aerosol single-scattering albedo: Measurements and model calculations for a coastal site near the Sea of Japan during ACE-Asia, *J. Geophys. Res.*, *108*(D23), 8648, doi:10.1029/2002JD003250.

Hong, Y. T., H. B. Zhang, Y. X. Zhu, H. C. Pu, H. B. Jiang, Y. Q. Zeng, and G. S. Liu (1992), Sulfur isotope compositions in China coal and sulfur isotope fractionation during coal combustion (in Chinese), *Chin. Sci.*, *8*, 868–873.

Hulston, J. R., and H. G. Thode (1965), Variations in the ^{33}S, ^{34}S, and ^{36}S contents of meteorites and their relation to chemical and nuclear effects, *J. Geophys. Res.*, *70*(14), 3475–3484, doi:10.1029/JZ070i014p03475.

Intergovernmental Panel on Climate Change (2007), *Climate Change 2007: The Physical Science Basis, a report accepted by Working Group I of the Intergovernmental Panel on Climate Change*, edited by J. T. Houghton et al., Cambridge Univ. Press, New York.

Johnston, D. T., et al. (2007), Sulfur isotope insights into microbial sulfate reduction: When microbes meet models, *Geochim. Cosmochim. Acta*, *71*(16), 3929–3947, doi:10.1016/j.gca.2007.05.008.

Kawamura, H., N. Matsuoka, S. Tawaka, and N. Momoshima (2001), Sulfur isotope variations in atmospheric sulfur oxides, particulate matter and deposits collected at Kyushu island, Japan, *Water Air Soil Pollut.*, *130*, 1775–1780, doi:10.1023/A:1013932724433.

Lasaga, A. C., T. Otake, Y. Watanabe, and H. Ohmoto (2008), Anomalous fractionation of sulfur isotopes during heterogeneous reactions, *Earth Planet. Sci. Lett.*, *268*, 225–238, doi:10.1016/j.epsl.2008.01.016.

Lee, C. C. W. (2000), Multiple stable oxygen isotopic studies of atmospheric sulfate: A new quantitative way to understand sulfate formation processes in the atmosphere, Ph.D. thesis, Univ. of Calif., San Diego, La Jolla.

Li, C., L. T. Marufu, R. R. Dickerson, Z. Q. Li, T. X. Wen, Y. S. Wang, P. C. Wang, H. B. Chen, and J. W. Stehr (2007), In situ measurements of trace gases and aerosol optical properties at a rural site in northern China during East Asian Study of Tropospheric Aerosols: An International Regional Experiment 2005, *J. Geophys. Res.*, *112*, D22S04, doi:10.1029/2006JD007592.

Li, X. D., H. Masuda, M. Ono, M. Kusakabe, F. Yanagisawa, and H. Zeng (2006), Contribution of atmospheric pollutants into groundwater in the northern Sichuan Basin, China, *Geochem. J.*, *40*, 103–119, doi:10.2343/geochemj.40.103.

Li, Z. (2004), Aerosol and climate: A perspective from East Asia, in *Observation, Theory, and Modeling of the Atmospheric Variability*, pp. 501–525, World Sci., Hackensack, N. J.

Li, Z., et al. (2007a), Aerosol optical properties and their radiative effects in northern China, *J. Geophys. Res.*, *112*, D22S01, doi:10.1029/2006JD007382.

Li, Z., et al. (2007b), Preface to special section on East Asian Studies of Tropospheric Aerosols: An International Regional Experiment (EAST-AIRE), *J. Geophys. Res.*, *112*, D22S00, doi:10.1029/2007JD008853.

Lyons, J. R. (2008), Photolysis of long-lived predissociative molecules as a source of mass-independent isotope fractionation: The example of SO_2, *Adv. Quantum Chem.*, *55*, 57–74, doi:10.1016/S0065-3276(07)00205-5.

Lyons, J. R. (2009), Atmospherically derived mass-independent sulfur isotope signatures, and incorporation into sediments, *Chem. Geol.*, *267*, 164–174, doi:10.1016/j.chemgeo.2009.03.027.

Ma, Z. Q., Y. S. Wang, Y. Sun, D. S. Ji, and B. Hu (2007), Characteristics of ozone and oxidation of nitrogen in Beijing and Xianghe (in Chinese), *Environ. Chem.*, *26*(6), 832–837.

Martins, J. V., P. Artaxo, Y. J. Kaufman, A. D. Castanho, and L. A. Remer (2009), Spectral absorption properties of aerosol particles from 350–2500 nm, *Geophys. Res. Lett.*, *36*, L13810, doi:10.1029/2009GL037435.

Mukai, H., et al. (2001), Regional characteristics of sulfur and lead isotope ratios in the atmosphere at several Chinese urban sites, *Environ. Sci. Technol.*, *35*, 1064–1071, doi:10.1021/es001399u.

Nielsen, H. (1974), Isotopic composition of the major contributions to atmospheric sulfur, *Tellus*, *26*, 213–221.

Norman, A. L., L. A. Barrie, D. Toom-Sauntry, A. Sirois, H. R. Krouse, S. M. Li, and S. Sharma (1999), Sources of aerosols sulfate at Alert: Apportionment using stable isotopes, *J. Geophys. Res.*, *104*(D9), 11,619–11,631, doi:10.1029/1999JD900078.

Norman, A., K. Anlauf, K. Hayden, B. Thompson, J. R. Brook, S. Li, and J. Bottenheim (2006), Aerosol sulfate and its oxidation on the pacific NW coast: S and O isotopes in PM2.5, *Atmos. Environ.*, *40*, 2676–2689, doi:10.1016/j.atmosenv.2005.09.085.

Novak, M., I. Jackova, and E. Prechova (2001), Temporal trends in the isotope signature of air-borne sulfur in central Europe, *Environ. Sci. Technol.*, *35*, 255–260, doi:10.1021/es0000753.

Oltmans, S. J., and D. J. Hofmann (1995), Increase in low-stratospheric water vapor at a mid-latitude Northern Hemisphere site from 1981 to 1994, *Nature*, *374*, 146–149, doi:10.1038/374146a0.

Ono, S., A. J. Kaufman, J. Farquhar, D. Y. Sumner, and N. J. Beukes (2009), Lithofacies control on multiple-sulfur isotope records and

Neoarchean sulfur cycles, *Precambrian Res.*, *169*, 58–67, doi:10.1016/j.precamres.2008.10.013.

Pavlov, A. A., M. J. Mills, and O. B. Toon (2005), Mystery of the volcanic mass-independent sulfur isotope fractionation signature in the Antarctic ice core, *Geophys. Res. Lett.*, *32*, L12816, doi:10.1029/2005GL022784.

Poulida, O., R. R. Dickerson, and A. Heymsfield (1996), Stratosphere-troposphere exchange in a midlatitude mesoscale convective complex, *J. Geophys. Res.*, *101*(D3), 6823–6836, doi:10.1029/95JD03523.

Prospero, J. M., D. L. Savoie, and R. Arimoto (2003), Long-term record of nss-sulfate and nitrate in aerosols on Midway Island, 1981–2000: Evidence of increased (now decreasing?) anthropogenic emissions from Asia, *J. Geophys. Res.*, *108*(D1), 4019, doi:10.1029/2001JD001524.

Qian, Y., D. P. Kaiser, L. R. Leung, and M. Xu (2006), More frequent cloud-free sky and less surface solar radiation in China from 1955 to 2000, *Geophys. Res. Lett.*, *33*, L01812, doi:10.1029/2005GL024586.

Quan, J. N., X. S. Zhang, Q. Zhang, J. H. Guo, and R. D. Vogt (2008), Importance of sulfate emission to sulfur deposition at urban and rural sites in China, *Atmos. Environ.*, *89*, 283–288.

Romero, A. B., and M. H. Thiemens (2003), Mass-independent sulfur isotopic compositions in present-day sulfate aerosols, *J. Geophys. Res.*, *108*(D16), 4524, doi:10.1029/2003JD003660.

Saltzman, E. S., G. Brass, and D. Price (1983), The mechanism of sulfate aerosol formation: Chemical and sulfur isotopic evidence, *Geophys. Res. Lett.*, *10*, 513–516, doi:10.1029/GL010i007p00513.

Savarino, J., A. Romero, J. Cole-Dai, S. Bekki, and M. H. Thiemens (2003), UV induced mass-independent sulfur isotope fractionation in stratospheric volcanic sulfate, *Geophys. Res. Lett.*, *30*(21), 2131, doi:10.1029/2003GL018134.

Stenchikov, G., R. Dickerson, K. Pickering, W. Ellis, B. Doddridge, S. Kondragunta, O. Poulida, J. Scala, and W. K. Tao (1996), Stratosphere-troposphere exchange in a midlatitude mesoscale convective complex: 2. Numerical simulations, *J. Geophys. Res.*, *101*(D3), 6837–6851, doi:10.1029/95JD02468.

Szynkiewicz, A., C. H. Moore, M. Glamoclija, and L. M. Pratt (2009), Sulfur isotope signatures in gypsiferous sediments of the Estancia and Tularosa Basins as indicators of sulfate sources, hydrological processes, and microbial activity, *Geochim. Cosmochim. Acta*, *73*(20), 6162–6186, doi:10.1016/j.gca.2009.07.009.

Takahashi, Y., T. Miyoshi, S. Yabuki, Y. Inada, and H. Shimizu (2008), Observation of transformation of calcite to gypsum in mineral aerosols by CaK-edge X-ray absorption near-edge structure (XANES), *Atmos. Environ.*, *42*, 6535–6541, doi:10.1016/j.atmosenv.2008.04.012.

Tanaka, N., and K. K. Turekian (1995), Determination of the dry deposition flux of SO_2 using cosmogenic ^{35}S and ^{7}Be measurements, *J. Geophys. Res.*, *100*(D2), 2841–2848, doi:10.1029/94JD02305.

Tanaka, N., D. M. Rye, Y. Xiao, and A. C. Lasaga (1994), Use of stable sulfur isotope systematics for evaluating oxidation reaction pathways and in-cloud scavenging of sulfur-dioxide in the atmosphere, *Geophys. Res. Lett.*, *21*, 1519–1522, doi:10.1029/94GL00893.

Thode, H. G., J. Monster, and H. B. Dunford (1961), Sulphur isotope geochemistry, *Geochim. Cosmochim. Acta*, *25*(3), 159–174, doi:10.1016/0016-7037(61)90074-6.

Torfs, K. M., and R. E. Van Grieken (1997), Use of stable isotope measurement to evaluate the origin of sulfur in gypsum layers on limestone building, *Environ. Sci. Technol.*, *31*, 2650–2655, doi:10.1021/es970067v.

Toyama, K., H. Satake, S. Takashima, T. Matsuda, M. Tsuruta, and K. Kawada (2007), Long-range transportation of contaminants from the Asian continent to the north Japan Alps, recorded in snow cover on Mt. Nishi-Hodaka-Dake, *Bull. Glaciol. Res.*, *24*, 37–47.

Ueno, Y., S. Ono, D. Rumble, and S. Maruyama (2008), Quadruple sulfur isotope analysis of ca. 3.5 Ga Dresser Formation: New evidence for microbial sulfate reduction in the early Archean, *Geochim. Cosmochim. Acta*, *72*(23), 5675–5691, doi:10.1016/j.gca.2008.08.026.

Wen, T. X., Y. S. Wang, and K. Zhang (2007), Study on sulfate and sulfur oxidation ratio in PM10 during heating season in Beijing (in Chinese), *J. Grad. Sch. Chin. Acad. Sci.*, *24*(5), 584–589.

Winterholler, B., P. Hoppe, J. Huth, S. Foley, and M. O. Andreae (2008), Sulfur isotope analysis of individual aerosol particles in the urban aerosol at a central European site (Mainz, Germany), *Atmos. Chem. Phys. Discuss.*, *8*, 9347–9404.

Xu, M., C.-P. Chang, C. Fu, Y. Qi, A. Robock, D. Robinson, and H. Zhang (2006), Steady decline of East Asian monsoon winds, 1969–2000: Evidence from direct ground measurements of wind speed, *J. Geophys. Res.*, *111*, D24111, doi:10.1029/2006JD007337.

Xu, Q. (2001), Abrupt change of the mid-summer climate in central east China by the influence of atmospheric pollution, *Atmos. Environ.*, *35*, 5029–5040, doi:10.1016/S1352-2310(01)00315-6.

Yu, H., S. C. Liu, and R. E. Dickinson (2002), Radiative effects of aerosols on the evolution of the atmospheric boundary layer, *J. Geophys. Res.*, *107*(D12), 4142, doi:10.1029/2001JD000754.

Zhang, H. B., A. Q. Hu, C. Z. Lu, and G. X. Zhang (2002), Sulfur isotopic composition of acid deposition in South China Regions and its environmental significance (in Chinese), *China Environ. Sci.*, *22*(2), 165–169.

Zmolek, P., X. P. Xu, T. Jackson, M. H. Thiemens, and W. C. Trogler (1999), Large mass independent sulfur isotope fractionations during the photopolymerization of (CS_2)-C-12 and (CS_2)-C-13, *J. Phys. Chem. A*, *103*, 2477–2480, doi:10.1021/jp9907140.

R. R. Dickerson, C. Li, and Z. Li, Department of Atmospheric and Oceanic Science, University of Maryland, College Park, MD 20740, USA. (zli@atmos.umd.edu)

J. Farquhar, A. J. Kaufman, and N. Wu, Department of Geology, University of Maryland, College Park, MD 20740, USA.

Z. Guo, School of Environmental Science and Engineering, Nanjing University of Information Science and Technology, 210044 Nanjing, China.

P. Wang, Institute of Atmospheric Physics, Chinese Academy of Sciences, Beijing 100029, China.